



Numerical predictions of aerosol charging and electrical conductivity of the lower atmosphere of Mars

M. Michael,¹ M. Barani,² and S. N. Tripathi¹

Received 18 October 2006; revised 28 November 2006; accepted 24 January 2007; published 28 February 2007.

[1] The charging of aerosols and the conductivity of the lower, night time atmosphere of Mars are calculated. The charge distribution of aerosols was obtained by the simultaneous solution of the ion-aerosol charge balance equations. Galactic cosmic rays are the dominant ionizing process in the night time lower atmosphere producing molecular ions and ion clusters. The ion production rates for different solar activities are considered. The ion-ion recombination rates and the ion-aerosols attachment coefficients are calculated for altitudes from 0 to 70 km. Both the steady state and time dependent concentration of charged aerosols are calculated. The conductivity produced by ion-attachment of aerosols was found to decrease by a factor of five yielding a value of about $4 \times 10^{-12} \text{ Ohm}^{-1} \text{ m}^{-1}$ close to the surface. The effect on the conductivity of the temperature vs. altitude and the aerosol density are also estimated. **Citation:** Michael, M., M. Barani, and S. N. Tripathi (2007), Numerical predictions of aerosol charging and electrical conductivity of the lower atmosphere of Mars, *Geophys. Res. Lett.*, 34, L04201, doi:10.1029/2006GL028434.

1. Introduction

[2] Several missions to Mars have passed through the Martian atmosphere and have carried out research on the surface, but there have been no measurements or modeling of the vertical conductivity of the lower atmosphere. In this region cosmic rays are the dominant ionizing mechanism for the night time Martian atmosphere. Some of the ions produced cause aerosol charging by attachment. This reduces the conductivity of the atmosphere as the conductivity is inversely proportional to the mass of the charge carrier. Since none of the missions to Mars included electrical instrumentation, the only experimental evidence for electrical activity is the electrostatic adhesion of dust to the wheels of the Mars Pathfinder and Sojourner rovers [Ferguson *et al.*, 1999].

[3] It is generally accepted that the global electric circuit is driven by thunderstorms on Earth. For a global electric circuit to exist on Martian atmosphere, a constant current generator must be present in a finitely conducting atmosphere. Cloud particles exist in the atmosphere of Mars at altitudes about 30 km [e.g., Montmessin *et al.*, 2006], and there may be thunderstorms too. Farrell and Desch [2001] have suggested that Mars possesses a global electric circuit

driven by dust storms. Therefore it is important to study the charging of particles and the conductivity of the atmosphere as there could be a driving force for a global electric circuit.

[4] Krauss *et al.* [2006] suggested that charge separation and electric-field breakdown are likely to occur in Martian dust storms. Theory, laboratory experiments, and field measurements on Earth suggest that the electrically charged Martian dust storms are potential hazards to Landers. The consequences of the development of a large-scale electric field on Mars are important in several areas like the transport of dust particles, as for micron size particles electrical forces may become comparable to the drag forces and surface material chemistry etc. It has also been suggested that the lightning and electrical discharges may influence the production of those chemical compounds that have been related to speculations regarding life on Mars.

[5] There have been observational and laboratory studies [Ferguson *et al.*, 1999; Sickafoose *et al.*, 2001] and numerical and analytical models [Melnik and Parrot, 1998; Farrell and Desch, 2001] of aerosol charging in the Martian atmosphere. Berthelier *et al.* [2000] reviewed various charging mechanisms operating in the Martian atmosphere. Most of these studies are focused on aerosols close to the surface. The present work calculates the aerosol charging for altitudes from 0 to 70 km which is then used to get the first estimate of the atmospheric conductivity.

[6] The current theories of aerosol charging are divided into three types [Yair and Levin, 1989]: (1) continuum theories treat the charging of particles with sizes larger than the ionic mean free path, (2) free molecular theories are applicable to particles much smaller than the ionic mean free path and (3) transition theories apply when the size of particles becomes comparable to the ionic mean free path. As the Martian atmosphere is tenuous, the ionic mean free path is comparable to the size of the aerosols close to the surface and is larger than the size of the aerosols at higher altitudes. Therefore free molecular theories and transition theories prevail in the lower atmosphere.

[7] As discussed by Yair and Levin [1989], charge balance equations can be used to calculate the steady-state ion concentrations and aerosol charge state. These equations are solved to obtain steady-state concentrations of positive and negative ions and charged aerosol particles. A similar procedure was recently used by Borucki *et al.* [2006] to calculate the electrical conductivity and charging of aerosols in the atmosphere of Titan. Ionization rates, ion-ion recombination coefficients and ion-aerosol attachment coefficients are described in the following section. These are used to calculate ion and aerosol concentrations

¹Department of Civil Engineering, Indian Institute of Technology, Kanpur, India.

²Department of Electrical Engineering, Indian Institute of Technology, Kanpur, India.

and the conductivity of the lower night time atmosphere of Mars.

2. Input Data

[8] To calculate the aerosol charging and ionic conductivity of the atmosphere it is necessary to choose a standard atmosphere. The density and temperature determine the mobility and the mean free path which in turn are essential in calculating the attachment coefficients and subsequently the conductivity. The Mars Pathfinder data for the northern summer neutral atmosphere were obtained from *Magalhaes et al.* [1999].

[9] Ionization rates are required to calculate the ion concentrations and therefore it is essential to consider the ionization processes. The detailed study of the lower atmosphere of Mars by *Molina-Cuberos et al.* [2001] has shown that the galactic cosmic rays are the major night-time ionization agent. K. O'Brien (private communication, 2005) has calculated the ion production rates at different altitudes for different solar activities and has shown that the maximum ion density occurs at the surface. The hydrated hydronium ion $\text{H}_3\text{O}^+(\text{H}_2\text{O})_4$ is the most abundant positive ion and the most abundant negative ion is $\text{CO}_3^-(\text{H}_2\text{O})_2$. These ions have mobilities which we calculated using the expression from *Borucki et al.* [1982]:

$$K = 3.74 \times 10^{20} (m\xi)^{-1/2} n^{-1} \quad (1)$$

Here n is the atmospheric number density, ξ is the polarizability of the neutrals and m is the ion-neutral reduced mass.

[10] In the night time lower atmosphere the aerosols become charged primarily by ion attachment. The rate at which steady-state is achieved in various ion environments requires absolute values of the ion-aerosol attachment coefficients and results in a statistical distribution of charge states. *Hoppel and Frick* [1986] have developed a method to calculate the attachment coefficients of ions to the aerosols which is used in the present study.

[11] The density and the size of the aerosols were estimated by *Chassefiere et al.* [1995] from the solar occultation measurements performed by the Auguste instrument onboard Phobos 2 spacecraft. *Chassefiere et al.* [1995] provided three different profiles for number density and effective radius of aerosols corresponding to three different values of the effective variance ($b = 0.1, 0.25, \text{ and } 0.4$) in particle size distribution. The present study used the one corresponding to the mean effective variance ($b = 0.25$), which is considered the standard dust profile. *Chassefiere et al.* [1995] estimated the optical depth as 0.1–0.3 corresponding to the standard dust profile.

[12] Mars aerosol studies with Mars Global Surveyor Thermal Emission Spectrometer during 1999–2001 have been reviewed by *Clancy et al.* [2003]. They suggested that the dust particle sizes vary with respect to latitudes, contrary to previous inferences [e.g., *Tomasko et al.*, 1999]. Unfortunately the vertical structure of these variations is not available and have not been included in the present model. *Montmessin et al.* [2006] presented the aerosol size distribution from the SPICAM ultraviolet instrument onboard Mars Express. It was found that the UV measurements for

aerosol particle size for altitudes greater than 55 km agree with the profile used in the present study, but for altitudes less than 55 km the size distribution obtained from the UV instrument is not accurate.

3. Numerical Scheme

[13] The formulation of the ion-aerosol attachment process is well known. Concentrations of ions can be found from the three-level probabilistic master equations. These constitute a set of $2p + 3$ simultaneous differential equations, p being the maximum number of elementary charges allowed on a particle [*Hoppel and Frick*, 1986; *Yair and Levin*, 1989]. In the present work the maximum number of charges is initially assumed to be 100. The ionic balance equations can be written as

$$\frac{dn^+}{dt} = q - \alpha n^+ n^- - \sum_i \left(\beta_1^{(i)} n^+ N^i \right) \quad (2)$$

$$\frac{dn^-}{dt} = q - \alpha n^+ n^- - \sum_i \left(\beta_2^{(i)} n^- N^i \right) \quad (3)$$

Here, α is the ion-ion recombination coefficient, q is the ion production rate, $\beta_j^{(i)}$ is the attachment coefficient for ions of polarity j (1 for positive and 2 for negative) to particles with charge i and N^i is the density of particles of charge i . The quantities q , α and β are assumed to vary with altitude. The value of q ranges from 5.03 to 0.0069 $\text{cm}^{-3} \text{s}^{-1}$ in the altitude region from 0 to 70 km. α varies in the range from 2.8×10^{-13} to $9.3 \times 10^{-13} \text{ m}^3 \text{ s}^{-1}$ over the same altitude range. The values of β are all of the order of ~ 8 at the surface and $-11 \text{ m}^3 \text{ s}^{-1}$ at 70 km. The terms in the sum in equations (2) and (3) represent ionic losses due to attachment to aerosols carrying $-p$ to $+p$ elementary charges. The corresponding equations for the charge on the aerosols are

$$\frac{dN^i}{dt} = \beta_1^{(i-1)} n^+ N^{(i-1)} + \beta_2^{(i+1)} n^- N^{(i+1)} - \beta_1^{(i)} n^+ N^i - \beta_2^{(i)} n^- N^i \quad (4)$$

The elementary charges on the aerosols are allowed to vary between plus and minus 100 and therefore there are 203 simultaneous differential equations for each altitude. The differential equations are solved using the 5th order Runge-Kutta method. This approach is used to solve the set of equations at 10 km altitude intervals using the charge conservation as a check on the calculations.

4. Results and Discussion

[14] The charge balance equations were solved for aerosols having a concentration and effective radius of 2.26 cm^{-3} and $1.9 \mu\text{m}$, respectively, at the surface. The charging of the aerosols depends on the ion-aerosol attachment coefficients and ion-ion recombination coefficients. As the attachment coefficients and the recombination coefficients are functions of altitude, the rate of charging of the aerosols also varies with altitude. The positive and negative ionic concentrations were considered equal, $(q/\alpha)^{0.5}$, initially.

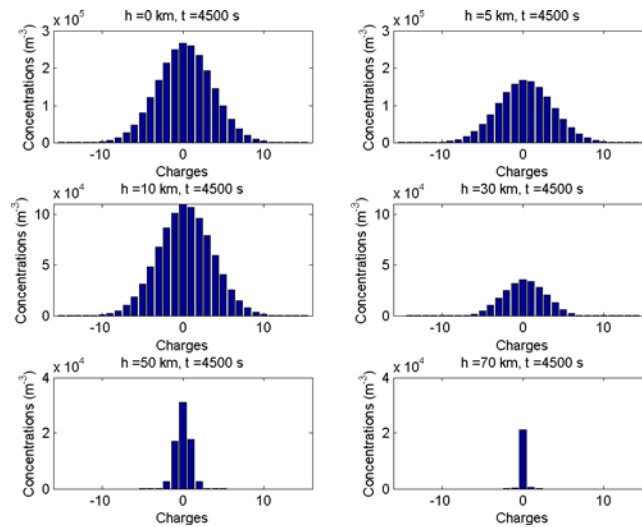


Figure 1. Steady state profile of charged aerosol concentration at altitudes 0, 5, 10, 30, 50 and 70 km.

At the beginning of the calculation aerosols are all neutral with charged aerosols produced due to the attachment of ions.

[15] Figure 1 presents the steady-state aerosol concentration for altitudes 0, 5, 10, 30, 50 and 70 km in the atmosphere. It is apparent that the concentration of charged aerosols decreases as the altitude increases. The aerosols are charged up to 36 (i.e. -36 and $+36$) at 0 km in the atmosphere, but at 70 km the aerosols are charged only up to ± 2 . The concentration of charged aerosols decreases as the charge on the aerosol increases. i.e. the neutral aerosols have maximum concentration and the aerosols with maximum charges have minimum concentration. It can also be noted that the steady-state concentration of the aerosols with positive charges is somewhat higher than the corresponding negatively charged aerosols. This is the case as the positive ions have higher mobility and are attached to the aerosols faster.

[16] Figure 2 presents the altitude profile of neutral as well as charged aerosols at steady-state. More than 80% of the neutral aerosols get charged close to the surface and almost none become charged at the upper boundary (70 km). This is due to the characteristics of the ion-aerosol attachment coefficients and the number density of the aerosols.

[17] The atmospheric conductivity depends on the existence of positive and negative ions, and the resulting conductivity can be expressed in terms of the number densities and mobilities of the individual charged species. In the lower atmosphere the conductivity is maintained by the small ions. The attachment of ions to aerosols reduces the conductivity as they become almost immobile by attachment to aerosol particles. The conductivity of the atmosphere is calculated as

$$\sigma = e \left(\sum_i n_{i+} K_{i+} + \sum_i n_{i-} K_{i-} \right) \quad (5)$$

where, e is the electronic charge, n is the number density of ions and K is the corresponding mobility, which is calculated using equation (1).

[18] In the case of Earth's atmosphere the conductivity increases above the ionization peak, which is approximately 10 km on average. For Mars the ionization peak occurs at the surface and the conductivity increases from the surface up to 70 km. This is due to less frequent collisions between ions and neutrals, which is a result of smaller number density. This, in turn, leads to smaller cluster size and the attachment rate. The number density of positive ions at the surface and at 70 km are 2.9×10^9 and $1.7 \times 10^8 \text{ m}^{-3}$ respectively, resulting in mobilities of 0.015 and $35 \text{ cm}^2 \text{V}^{-1} \text{s}^{-1}$. Whereas the density decreases by an order of magnitude in going from 0 to 70 km, the mobility increases by more than 3 orders of magnitude. The presence of aerosols decreases the conductivity by vastly increasing the mass of the charge carriers. As aerosols are present in greater quantities closer to the surface, the conductivity closer to the surface is lowered dramatically as indicated by the solid line in Figure 3.

[19] To understand the effect of the aerosols, the atmospheric conductivity is calculated without aerosols in the

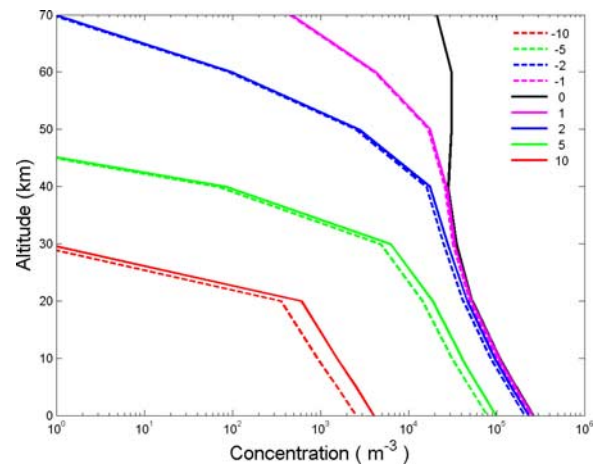


Figure 2. Altitude profile of the aerosols with charges 0, 1, 2, 5 and 10 at steady-state. The dashed lines represent the negatively charged and solid lines represent the positively charged aerosols.

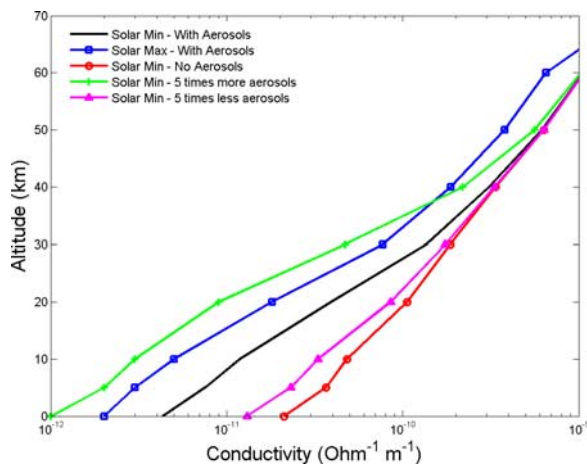


Figure 3. Conductivity of the lower atmosphere of Mars. The solid line represents the conductivity calculated for ion production rate at solar minimum conditions. Line with squares represents the conductivity calculated for ion production rate at solar maximum conditions. The lines with pluses and triangles represent the conductivity with 5 times more and 5 times less aerosols respectively. The line with circles represents the conductivity in the absence of aerosols.

atmosphere and the result is presented in Figure 3 as the line with circles. It was found that the conductivity dropped by about a factor of five close to the surface in the presence of aerosols. As fewer ions get attached to aerosols at higher altitudes, the difference in conductivity with and without aerosols is almost negligible at the upper boundary (70 km).

[20] The Mars Global Surveyor radio science instrument has observed the temperature structure of the southern hemisphere in summer. To study the effect of the temperature structure on the conductivity, the above calculations have also been carried out using this temperature profile, which shows an inversion at 10 km and then decreases with altitude and becomes similar to that in the northern summer at the upper boundary (70 km). The difference observed in the conductivity due to the different temperature structures is less than 5%. The temperature structure for different seasons and latitudes were considered and the one mentioned above showed maximum variation from the one observed by Mars Pathfinder in the Northern summer. Therefore it is apparent that the variation in conductivity due to different temperature structures is very small.

[21] As the ion production rate by cosmic rays varies with solar activity, we studied the effect of solar activity on the aerosol charging and the conductivity. The conductivity calculated for the solar maximum condition is presented in Figure 3 as the line with squares. It was found that there was a difference of about a factor of two in the conductivity between solar maximum and minimum conditions due to the fact that the ion production rate by cosmic rays is maximum during solar minimum conditions and vice versa. The atmospheric conductivity can also vary daily due to the presence of solar radiation during the day which can ionize gases [Grard, 1995] and yearly, due to the global atmospheric pressure variations. The results of these variations will be presented in a subsequent paper.

[22] The conductivities are calculated for different values of dust density and size corresponding to the extreme effective variance ($b = 0.1$ and $b = 0.4$) in particle size distribution [Chassefiere *et al.*, 1995]. The conductivity decreases by a factor of two at the surface for $b = 0.1$ and increases by a factor of two for $b = 0.4$. At the upper boundary the conductivities were within 1% of each other. For $b = 0.1$, the number density at the surface is about a factor of two less and for $b = 0.4$ it is about a factor of two greater than that of $b = 0.25$. The effective radius is about 7% less and for $b = 0.1$ and is about 7% greater for $b = 0.4$ than that for $b = 0.25$ at the surface.

[23] To understand the effect of dust concentration, the conductivity is calculated for a number of aerosol concentrations. It was found that the conductivity decreased by about a factor of four when the aerosol concentration was increased by a factor of five and the conductivity increased by a factor of more than three when the aerosol concentration was reduced by a factor of five at the surface. At the top boundary the conductivity was only marginally affected by reasonable variations in the concentration. In Figure 3 the line with pluses represents the conductivity with five times more aerosols and the line with triangles represents the conductivity with five times less aerosols. It was observed that the optical depth is within 2–5 during dust storms [Read and Lewis, 2004]. The conductivity decreases by about an order of magnitude at the surface when the optical depth is increased to ~ 3 . The ionization peak may also vary with the dust loading, however, we have not studied its sensitivity to aerosol concentration.

[24] In the daytime Martian atmosphere, solar UV photons can reach the surface producing additional photoelectrons at all altitudes. These photoelectrons contribute to the atmospheric conductivity and Berthelier *et al.* [2000] and Grard [1995] suggested that the best estimate of the conductivity at the surface is in the range $\sim 10^{-12}$ – 10^{-10} $\text{Ohm}^{-1} \text{m}^{-1}$. In the present work we calculated the night time conductivity and found that the conductivity at the surface is $\sim 4 \times 10^{-12}$ $\text{Ohm}^{-1} \text{m}^{-1}$, which is within the predicted range.

5. Conclusions

[25] Following are the important conclusions of the present study of the night time conductivity of the lower Martian atmosphere:

[26] 1. more aerosols (about 80%) become charged closer to the surface than at higher altitudes;

[27] 2. the charge state of the aerosols at lower altitudes is higher (up to ± 36);

[28] 3. the variation of the night time conductivity is less than 5% due to the differences in the seasonal and latitudinal temperature structure;

[29] 4. the conductivity varies by about a factor of two in going from solar minimum to solar maximum conditions;

[30] 5. the conductivity changes by a factor of 3–4 for a change of a factor of 5 in the aerosol concentration; and

[31] 6. when the atmospheric opacity due to an increase in aerosol density is increased to ~ 3 , the conductivity at the surface is reduced by almost an order of magnitude.

[32] A decrease in conductivity indicates that space charge is residing on particles. When there is large popula-

tion of highly charged particles, the discharge mechanism also becomes more effective, which can produce lightning etc. The present calculations are made for the night time Martian atmosphere. The daytime conductivity which includes the solar EUV radiation is being studied. Grard [1995] have estimated that the solar EUV photons with energies up to 6 eV penetrate the atmosphere of Mars and emit electrons from aerosols of the lower atmosphere of Mars. Presently the equations are solved only for mono-dispersed aerosols. Polydisperse aerosols are also being included in the simulations that are in progress.

[33] **Acknowledgments.** The authors acknowledge support of Indian Space Research Organisation Planex program. The authors gratefully acknowledge the ionization rate profiles provided by Karen O'Brien.

References

- Berthelot, J. J., R. Grard, H. Laakso, and M. Parrot (2000), ARES atmospheric relaxation and electric field sensor, the electric field experiment on NETLANDER, *Planet. Space Sci.*, *48*, 1183–1200.
- Borucki, W. J., Z. Levin, R. C. Whitten, R. G. Keesee, L. A. Capone, O. B. Toon, and J. Dubach (1982), Predicted electrical conductivity between 0 and 80 km in the Venusian atmosphere, *Icarus*, *51*, 302–321.
- Borucki, W. J., R. C. Whitten, E. L. O. Bakes, E. Barth, and S. Tripathi (2006), Predictions of the electrical conductivity and charging of the aerosols in Titan's atmosphere 6/20/05, *Icarus*, *181*, 527–544.
- Chassefiere, E., P. Drossart, and O. Korabiev (1995), Post-Phobos model for the altitude and size distribution of dust in the low Martian atmosphere, *J. Geophys. Res.*, *100*, 5525–5539.
- Clancy, R. T., M. J. Wolff, and P. R. Christensen (2003), Mars aerosol studies with the MGS TES emission phase function observations: Optical depths, particle sizes, and ice cloud types versus latitude and solar longitude, *J. Geophys. Res.*, *108*(E9), 5098, doi:10.1029/2003JE002058.
- Farrell, W. M., and M. D. Desch (2001), Is there a Martian atmospheric electric circuit?, *J. Geophys. Res.*, *106*, 7591–7595.
- Ferguson, D. C., L. C. Kolecki, M. W. Siebert, D. M. Wilt, and J. R. Matijevic (1999), Evidence from Martian electrostatic charging and abrasive wear from the Wheel Abrasion Experiment on the Pathfinder Sojourner rover, *J. Geophys. Res.*, *104*, 8747–8759.
- Grard, R. (1995), Solar photon interaction with the Martian surface and related electrical and chemical phenomena, *Icarus*, *114*, 130–138.
- Hoppel, W. A., and G. M. Frick (1986), Ion-aerosol attachment coefficients and the steady-state charge distribution on aerosols in a bipolar ion environment, *Aerosol Sci. Technol.*, *5*, 1–21.
- Krauss, C. E., M. Horányi, and S. Robertson (2006), Modeling the formation of electrostatic discharges on Mars, *J. Geophys. Res.*, *111*, E02001, doi:10.1029/2004JE002313.
- Magalhaes, J. A., J. T. Schofield, and A. Seiff (1999), Results of the Mars Pathfinder atmospheric structure investigation, *J. Geophys. Res.*, *104*, 8943–8955.
- Melnik, O., and M. Parrot (1998), Electrostatic discharge in Martian dust storms, *J. Geophys. Res.*, *103*, 29,107–29,117.
- Molina-Cuberos, G. J., J. J. Lopez-Moreno, R. Rodrigo, H. Lichtenegger, and K. Schwingenschuh (2001), A model of the Martian ionosphere below 70 km, *Adv. Space Res.*, *27*, 1801–1806.
- Montmessin, F., E. Quémerais, J. L. Bertaux, O. Korabiev, P. Rannou, and S. Lebonnois (2006), Stellar occultations at UV wavelengths by the SPICAM instrument: Retrieval and analysis of Martian haze profiles, *J. Geophys. Res.*, *111*, E09S09, doi:10.1029/2005JE002662.
- Read, P. L. and S. R. Lewis (2004), Dust storms, devils, and transport, in *The Martian Climate Revisited*, Springer Praxis Books Geophys. Sci., edited by P. L. Read, pp. 179–217, Springer, New York.
- Sickafoose, A. A., J. E. Colwell, M. Horányi, and S. Robertson (2001), Experimental investigation on photoelectric and triboelectric charging of dust, *J. Geophys. Res.*, *106*, 8343–8356.
- Tomasko, M. G., L. R. Doose, M. Lemmon, P. H. Smith, and E. Wegryn (1999), Properties of dust in the Martian atmosphere from the Imager on Mars Pathfinder, *J. Geophys. Res.*, *104*, 8987–9008.
- Yair, Y., and Z. Levin (1989), Charging of polydispersed aerosol particles by attachment of atmospheric ions, *J. Geophys. Res.*, *94*, 13,085–13,091.

M. Barani, Department of Electrical Engineering, Indian Institute of Technology, Kanpur 208016, India.

M. Michael and S. N. Tripathi, Department of Civil Engineering, Indian Institute of Technology, Kanpur 208016, India. (snt@iitk.ac.in)